PERGAMON

International Journal of Solids and Structures 39 (2002) 89–104

INTERNATIONAL JOURNAL OF SOLIDS and STRUCTURES

www.elsevier.com/locate/ijsolstr

Non-uniform frictional sliding under cyclic loading with frictional characteristics changing in the process of sliding

Larissa Gorbatikh [a], Boris Nuller [b], Mark Kachanov [c,*]

[a] *Department of Mechanical Engineering, University of New Mexico, Albuquerque, NM 87131, USA*
[b] *Department of Mathematics, Academy of Forest Technologies, St.-Petersburg, 195 220 Russia*
[c] *Department of Mechanical Engineering, Tufts University, 204 Anderson Hall, Medford, MA 02155, USA*

Received 16 December 2000

Abstract

Frictional sliding on a crack with non-uniform frictional characteristics is considered. The present work continues the investigation of Gorbatikh et al. [Int. J. Solids Struct., in press] and focuses on the cyclic loading. The evolution of the sliding process in loading–reloading–unloading cycles is analyzed. We also extend the analysis to the important case when the frictional resistance changes in the process of sliding (such changes may model "degradation" of the sliding surface during sliding, as well as other physical factors, not necessarily related to the sliding itself). © 2001 Published by Elsevier Science Ltd.

Keywords: Friction; Crack; Sliding; Cyclic loading

1. Introduction

The problem of a crack that has non-uniform frictional characteristics along it and undergoes partial, gradually spreading, sliding under applied compression and shear is considered. This may model situations with local changes of frictional resistance (due to local drops/elevations in normal stresses, local lubrications, etc.) that are relevant for a number of applications (like rotating machinery with frictional contacts). They are particularly important for the geological fracture mechanics. Field observations and seismic data indicate that the slip distributions along the geological faults are quite complex and non-uniform (Pollard and Segall, 1980; Rudnicki and Kanamori, 1981; Cooke, 1997; Schultz, 1999). The analysis is also relevant for the proper interpretation of experimental data on frictional sliding (Marone, 1998).

The present work continues the investigation of Gorbatikh et al. (in press) and focuses on cyclic loading. It also extends the analysis to the important case when the frictional resistance changes in the process of sliding (such changes may model "degradation" of the sliding surface during sliding, as well as other physical factors, not necessarily related to the sliding itself). We study the hysteresis and the "memory" of

* Corresponding author. Tel.: +1-617-627-3318; fax: +1-617-627-3058.
E-mail address: mark.kachanov@tufts.edu (M. Kachanov).

0020-7683/01/$ - see front matter © 2001 Published by Elsevier Science Ltd.
PII: S0020-7683(01)00171-8

the stress history under loading cycles, the dependence of reverse sliding at "unloading" on the amount of sliding accumulated during the previous stress cycle.

An important part of our analysis is that the crack may contain open (traction free) intervals. Such intervals model the situations when some material "fell off", so that contact between the crack faces is partially lost.

As far as cyclic loading of a non-uniform contact is concerned, earlier works should be mentioned. Weertman (1964) considered the case of one local minimum of frictional resistance in the simple form of a symmetric, piecewise constant function, under the cyclic loading. His work addresses the propagation of sliding but does not consider the distribution of slip (the displacement of discontinuity profile). Olsson (1984) considered an interval of local minimum of frictional resistance in the form of a symmetric "triangular" drop. He analyzed the propagation of sliding and the distribution of slip under the condition that sliding has not spread beyond the mentioned interval. These two works do not cover the possibilities that "open" (traction free) intervals may be present, or that the frictional resistance may change in the process of sliding.

2. Formulation of the problem

The formulation of the problem of non-uniform sliding, given by Gorbatikh et al. (in press) for the monotonic loading, is extended here for the cyclic loading paths. Thus, we consider an infinite two-dimensional solid with a crack $(-l, l)$ along the x-axis. Stresses at infinity (applied loads) are

$$\sigma_{yy} = \sigma_{yy}^{\infty(S)} < 0 \quad \text{and} \quad \sigma_{xy} = \sigma_{xy}^{\infty(S)} \tag{2.1}$$

where index S denotes a step of the loading history, according to the rule:

$$S = \begin{cases} 0, 2, 4, \ldots & \text{if } \mathrm{d}\sigma_{xy}^{\infty(S)} > 0 \quad \text{(loading)} \\ 1, 3, 5, \ldots & \text{if } \mathrm{d}\sigma_{xy}^{\infty(S)} < 0 \quad \text{(unloading)} \end{cases} \tag{2.2}$$

Frictional resistance is assumed to be variable along the crack (a function of x) and, in general, also may change during the sliding process (a function of S): $\tau^{(S)} = \tau^{(S)}(x)$. As a special case, it may be modeled by Coulomb's law $\tau^{(S)}(x) = -\mu^{(S)}(x)\sigma_{yy} + c^{(S)}(x)$ (where $\mu^{(S)}(x)$ and $c^{(S)}(x)$ are the coefficients of friction and cohesion, respectively), but our analysis is not restricted to this law.

The crack may experience four different regimes along its surface: intervals undergoing frictional sliding $L_1^{(S)}$, "locked" intervals $L_2^{(S)}$ without any previously accumulated sliding ($[u_x] = 0$), open (traction free) intervals $L_3^{(S)}$ and intervals $L_4^{(S)}$ with "locked" accumulation of sliding ($[u_x] \neq 0$) (schematically shown in Fig. 1). We note that the first three regimes were introduced in the earlier analysis of Gorbatikh et al. (in press) of the "monotonic" sliding, whereas the fourth regime, identified here, is due to the loading reversal.

The mentioned four regimes are defined by the following boundary conditions (brackets [ ] denote discontinuities of the corresponding quantities):

1. Along the set $L_1^{(S)}$ of *frictionally sliding* intervals

$$(-1)^S \sigma_{xy} = \tau^{(S)}(x), \quad [u_y] = 0, \quad [\sigma_{xy}] = [\sigma_{yy}] = 0 \quad \text{for } x \in L_1^{(S)} \tag{2.3a}$$

subject to the inequality

$$\sigma_{yy} < 0 \quad \text{for } x \in L_1^{(S)} \tag{2.3b}$$

2. Along the set $L_2^{(S)}$ of *locked* intervals that have not experienced any previous sliding:

$$[u_x] = [u_y] = 0, \quad [\sigma_{xy}] = [\sigma_{yy}] = 0 \quad \text{for } x \in L_2^{(S)} \tag{2.4a}$$

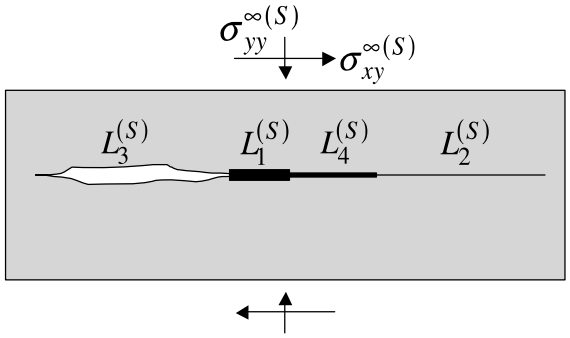

Fig. 1. Crack line comprising a sliding interval $L_1^{(S)}$ a "locked" interval without previous sliding $L_2^{(S)}$, an "open" interval $L_3^{(S)}$ and an interval $L_4^{(S)}$ with locked accumulation of sliding. Each of the intervals may actually consist of several subintervals.

subject to the inequalities

$$\sigma_{yy} < 0, \qquad (-1)^S \sigma_{xy} < \tau^{(S)}(x) \quad \text{for } x \in L_2^{(S)} \tag{2.4b}$$

3. Along the set $L_3^{(S)}$ of *open* (traction free) intervals

$$\sigma_{xy} = \sigma_{yy} = 0 \quad \text{for } x \in L_3^{(S)} \tag{2.5a}$$

The condition of non-overlapping of crack faces should also be imposed:

$$[u_y] \geqslant 0 \quad \text{for } x \in L_3^{(S)} \tag{2.5b}$$

or, in a more general case of a certain finite initial crack opening $\Delta(x)$ along $L_3^{(S)}$,

$$\Delta + [u_y] \geqslant 0 \tag{2.5c}$$

4. Along the set $L_4^{(S)}$ of intervals where a certain accumulated slip is locked:

$$[u_x] = \delta^{(S)}(x), \quad [u_y] = 0, \quad [\sigma_{xy}] = [\sigma_{yy}] = 0 \quad \text{for } x \in L_4^{(S)} \tag{2.6a}$$

($\delta^{(S)}(x)$ is a slip distribution that has accumulated in the previous sliding along $L_4^{(S)}$), with the following inequalities to be satisfied:

$$\sigma_{yy} < 0, \qquad (-1)^S \sigma_{xy} < \tau^{(S)}(x) \quad \text{for } x \in L_4^{(S)} \tag{2.6b}$$

The points that separate intervals of sliding $L_1^{(S)}$ from the locked intervals $L_2^{(S)}$ and $L_4^{(S)}$ are determined from the following condition for the stress intensity factor (SIF)

$$K_{\mathrm{II}} = 0 \tag{2.7}$$

(indeed, $K_{\mathrm{II}} \neq 0$ at the end point of $L_1^{(S)}$ and $L_4^{(S)}$ would have generated a singularity of shear stress σ_{xy} in $L_1^{(S)}$ and $L_4^{(S)}$, thus producing sliding there). At the tips $x = \pm l$ of the crack, Eq. (2.7) should be replaced by $K_{\mathrm{II}} < K_{\mathrm{IIC}}$, where K_{IIC} is a material constant (we do not consider a further development of the sliding process, when K_{II} exceeds K_{IIC} at the crack tips).

We now overview the general features of the sliding process in one loading cycle. The sliding process at the *first loading* ($S = 0$) starts at points of local minima of $\tau^{(0)}(x)$ and then propagates along the crack, as applied load $\sigma_{xy}^{\infty(0)}$ is increased. The crack experiences, generally, three regimes: sliding zones $L_1^{(0)}$, locked zones $L_2^{(0)}$ and open intervals $L_3^{(0)}$.

Let now the *unloading* process ($S = 1$) start at stress $\sigma_{xy^*}^{\infty(0)}$ where the first loading ended. At this point $L_1^{(1)} = 0$, $L_2^{(1)} = L_2^{(0)}$, $L_3^{(1)} = L_3^{(0)}$ and $L_4^{(1)} = L_1^{(0)}$, with the locked accumulation of sliding $[u_x] = \delta^{(1)}(x)$ to be

found from the solution of the problem for the preceding stage ($S = 0$). Reverse sliding starts when $-\sigma_{xy} = \tau^{(1)}(x)$, where $\tau^{(1)}(x)$ is the profile of frictional resistance during unloading. We assume that, generally, profiles $\tau^{(1)}(x)$ and $\tau^{(0)}(x)$ do not coincide, i.e. that the profile may be affected by sliding (''surface degradation''). If local minimums of $\tau^{(1)}(x)$ coincide with the ones of $\tau^{(0)}(x)$, the reverse sliding zones $L_1^{(1)}$ are contained within $L_4^{(1)}$ intervals; they propagate as the unloading progresses, whereas the locked intervals $L_4^{(1)}$ and $L_2^{(1)}$ shrink.

Let now the *reloading* process start at $\sigma_{xy^*}^{\infty(1)}$ ($S = 2$). At this point $L_1^{(2)} = 0$, $L_2^{(2)} = L_2^{(1)}$, $L_3^{(2)} = L_3^{(1)}$ and $L_4^{(2)} = L_1^{(1)} \cup L_4^{(1)}$ with the locked accumulation of sliding $[u_x] = \delta^{(2)}(x)$, to be found from the solution of the problem for the preceding stage ($S = 1$). New sliding zones $L_1^{(2)}$ nucleate when $\sigma_{xy} = \tau^{(2)}(x)$ and then propagate as $\sigma_{xy}^{\infty(2)}$ is increased.

Generally, at the point of reversal of the loading direction ($S - 1 \to S$) the following conditions hold:

$$L_1^{(S)} = 0, \quad L_2^{(S)} = L_2^{(S-1)}, \quad L_3^{(S)} = L_3^{(S-1)}, \quad L_4^{(S)} = L_1^{(S-1)} \cup L_4^{(S-1)} \tag{2.8}$$

$$\delta^{(S)}(x) = \begin{cases} \delta^{(S-1)}(x), & x \in L_4^{(S-1)} \\ [u_x^{(S-1)}], & x \in L_1^{(S-1)} \end{cases} \tag{2.9}$$

3. General solution in absence of open intervals

We first consider the case when there are no ''open'' (traction free) intervals $L_3^{(S)}$ and the crack line comprises interval(s) $L_1^{(S)}$ of frictional sliding, possibly alternating with locked interval(s) $L_2^{(S)}$ and intervals $L_4^{(S)}$ with locked accumulation of sliding from the preceding loading stage.

Following the usual formalism of two-dimensional elasticity, the solution is sought in terms of Kolosov–Muskhelishvili's potentials:

$$2G(u_x + \mathrm{i}u_y)' = \kappa\Phi(z) - \Phi(\bar{z}) - (z - \bar{z})\overline{\Phi'(z)} \tag{3.1a}$$

$$\sigma_{yy} - \mathrm{i}\sigma_{xy} = \Phi(z) + \Phi(\bar{z}) + (z - \bar{z})\overline{\Phi'(z)} \tag{3.1b}$$

where G is the shear modulus, $\kappa = 3 - 4\nu$ for plane strain and $\kappa = (3 - \nu)/(1 + \nu)$ for plane stress (ν is Poisson's ratio) and functions $\Phi(z)$, $\overline{\Phi}(z)$, defined by the relation $\overline{\Phi}(z) \equiv \overline{\Phi(\bar{z})}$, are piecewise analytic, with $L_1^{(S)}$, and $L_4^{(S)}$ being the discontinuity lines.

Using Eq. (3.1a), we obtain the following boundary condition on $L_4^{(S)}$:

$$2G(u_x^+ - u_x^-)' = (\kappa + 1)(\Phi^+(x) - \Phi^-(x)) = 2G\delta^{(S)'}(x) \tag{3.2a}$$

or

$$\Phi^+(x) - \Phi^-(x) = \frac{2G\delta^{(S)'}(x)}{\kappa + 1}, \quad x \in L_4^{(S)} \tag{3.2b}$$

According to Eq. (3.1b) $\sigma_{xy} = \mathrm{i}(\Phi^+(x) + \Phi^-(x))$ and boundary condition (2.3a) can be restated in terms of $\Phi(z)$ as follows:

$$\Phi^+(x) + \Phi^-(x) = (-1)^{S+1}\tau^{(S)}(x)\mathrm{i}, \quad x \in L_1^{(S)} \tag{3.3}$$

Thus, we have Riemann's problem (3.2a), (3.2b) and (3.3) for function $\Phi(z)$, with conditions at infinity that follow from Eq. (2.1).

We represent the problem as a superposition of two subproblems (Fig. 2). Subproblem (A) coincides with the problem (AA) considered at the preceding loading stage and its solution is assumed to be known.

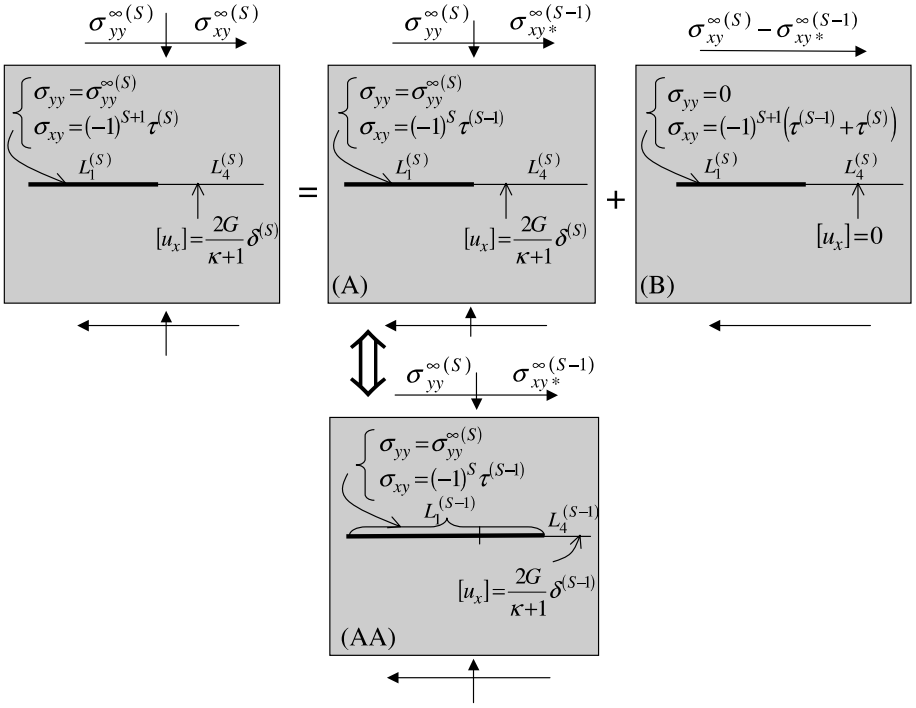

Fig. 2. Stress superposition for a crack comprising intervals $L_1^{(S)}$, $L_2^{(S)}$ and $L_4^{(S)}$.

Subproblem (B), where slip along $L_1^{(S)}$ is zero, was discussed in detail by Gorbatikh et al. (in press); it is briefly overviewed in the text to follow.

Assuming that, in the general case, the sliding zone $L_1^{(S)}$ comprises n sliding subintervals $L_1^{(S)(k)}$, with yet unknown endpoints $a_k^{(S)}$, $b_k^{(S)}$ (alternating with locked subintervals of $L_2^{(S)}$), we have the following expression for the complex potential $\Phi(z)$ (see, for example, Muskhelishvili (1953)):

$$\Phi(z) = \frac{1}{2\pi X(z)} \int_{L_1^{(S)}} \frac{X(t)\sigma_{xy}(t)\,\mathrm{d}t}{t-z} + \mathrm{i}\frac{P_n(z)}{X(z)} \tag{3.4}$$

where

$$X(z) = \sqrt{(z-a_1^{(S)})(z-b_1^{(S)})\cdots(z-a_n^{(S)})(z-b_n^{(S)})} \tag{3.5}$$

with the branch chosen in such a way that $z^{-n}X(z) \to 1$ as $z \to \infty$ (hence $X^+(t) = X(t)$ and $X^-(t) = -X(t)$ on $L_2^{(S)}$, where t is the coordinate along x-axis),

$$\sigma_{xy} = \sigma_{xy}^{\infty(S)} - \sigma_{xy^*}^{\infty(S-1)} - (-1)^{S+1}\left(\tau^{(S)}(x) + \tau^{(S-1)}(x)\right) \tag{3.6}$$

and where $P_n(z)$ is a polynomial of degree $\leqslant n$:

$$P_n(z) = C_0 z^n + C_1 z^{n-1} + \cdots + C_n \tag{3.7}$$

with real coefficients to be found from n conditions of uniqueness of displacements at points $a_k^{(S)}$ and $b_k^{(S)}$:

$$\oint_{A_1^{(S)(k)}} \Phi(z)\,\mathrm{d}z = 0, \quad (k = 1, \ldots, n) \tag{3.8}$$

where $\Lambda_1^{(S)(k)}$ are closed contours encircling $L_1^{(S)(k)}$. The SIFs entering the condition (2.7) and forming $2n$ equations for finding unknown endpoints $a_k^{(S)}$, $b_k^{(S)}$ are calculated in the usual way (for example, $K_{\mathrm{II}}(b_k) = \lim_{z\to b_k}(z-b_k)^{1/2}\Phi(z)$).

Thus, we reduced the original problem to two subproblems (A) and (B), where the solution of subproblem (A) is known from the previous stage and the solution of subproblem (B) can be found by the method described above.

4. Analysis in absence of open intervals

We consider the case of piecewise constant distribution of the frictional resistance $\tau^{(S)}(x)$ with one local minimum:

$$\tau^{(S)}(x) = \begin{cases} \tau_1^{(S)}, & a < x < b \\ \tau_2^{(S)}, & b < x < l \\ \tau_3^{(S)}, & -l < x < a \end{cases} \tag{4.1}$$

where $\tau_1^{(S)} \leqslant \tau_2^{(S)} \leqslant \tau_3^{(S)}$. Using this case, as well as the modified profile (4.3), we examine the typical features of the sliding process under cyclic loading.

4.1. Propagation of sliding and slip accumulation

The problem of propagation of the sliding zone (in terms of applied loads) can, in this case, be solved in elementary functions. We consider one loading cycle.

Loading from the initial state $\sigma_{xy}^{\infty(0)} = 0$ to a certain $\sigma_{xy^*}^{\infty(0)}$ $(S = 0)$. The entire crack is locked until the applied load reaches a critical level $\sigma_{xy}^{\infty(0)} = \tau_1^{(0)}$, at which point sliding occurs in the entire interval $a < x < b$ of lowest frictional resistance. As $\sigma_{xy}^{\infty(0)}$ is increased, sliding propagates into adjacent intervals $(a-\varepsilon_3^{(0)}, a)$ and $(b, b+\varepsilon_2^{(0)})$. Equating

$$K_{\mathrm{II}}\left\{ \begin{matrix} a-\varepsilon_3^{(0)} \\ b+\varepsilon_2^{(0)} \end{matrix} \right\}$$

to zero yields the following two equations for the endpoints $\varepsilon_2^{(0)}$ and $\varepsilon_3^{(0)}$:

$$\sigma_{xy}^{\infty} = \frac{\tau_2+\tau_3}{2} + \frac{\tau_2-\tau_1}{\pi}\arcsin\frac{s(1-\alpha_2^2)-1}{s(1+\alpha_2)^2-1} - \frac{\tau_3-\tau_1}{\pi}\arcsin\frac{s(1+\alpha_2)^2-2\alpha_2-1}{s(1+\alpha_2)^2-1}$$
$$\alpha_3 = s\alpha_2 + s - 1 \tag{4.2}$$

where $s = ((\tau_3-\tau_1)/(\tau_2-\tau_1))^2$, $\alpha_k = (b-a)\varepsilon_k^{-1}$ and $\tau_k = \tau_k^{(0)}$, $\varepsilon_k = \varepsilon_k^{(0)}$, $\sigma_{xy}^{\infty} = \sigma_{xy}^{\infty(0)}$. Numerical solution of Eq. (4.2) is illustrated in Fig. 3a and the corresponding slip distribution is shown in Fig. 4a.

Unloading from the state $\sigma_{xy}^{\infty(1)} = \sigma_{xy^*}^{\infty(0)}$ to $\sigma_{xy^*}^{\infty(1)}$ $(S = 1)$. No sliding occurs until the applied shear load drops to the level $\sigma_{xy}^{\infty(1)} = \sigma_{xy^*}^{\infty(0)} - (\tau_1^{(1)}(x) + \tau_1^{(0)}(x))$, at which point the reverse sliding occurs within (a, b). As $\sigma_{xy}^{\infty(1)}$ is further decreased, the reverse sliding propagates into adjacent intervals $(a-\varepsilon_3^{(1)}, a)$, $(b, b+\varepsilon_2^{(1)})$. The endpoints, $\varepsilon_2^{(1)}$ and $\varepsilon_3^{(1)}$ can be found from Eq. (4.2) by setting $\tau_k = \tau_k^{(0)} + \tau_k^{(1)}$, $\varepsilon_k = \varepsilon_k^{(1)}$ and $\sigma_{xy}^{\infty} = \sigma_{xy^*}^{\infty(0)} - \sigma_{xy}^{\infty(1)}$. Intervals $(a-\varepsilon_3^{(0)}, a-\varepsilon_3^{(1)})$ and $(b+\varepsilon_2^{(1)}, b+\varepsilon_2^{(0)})$ remain locked, with the amount of slip accumulated during the previous stage. Figs. 3b and 4b illustrate propagation of the reverse sliding zone and of the slip distribution, respectively. Note that, at the point when the system is unloaded $(\sigma_{xy}^{\infty(1)} = 0)$ a certain amount of residual slip still remains, although it is somewhat reduced (Fig. 4b, dotted line). Further reduction in the applied loads (resulting in negative $\sigma_{xy}^{\infty(1)}$) leads to expansion of the zone of reverse sliding

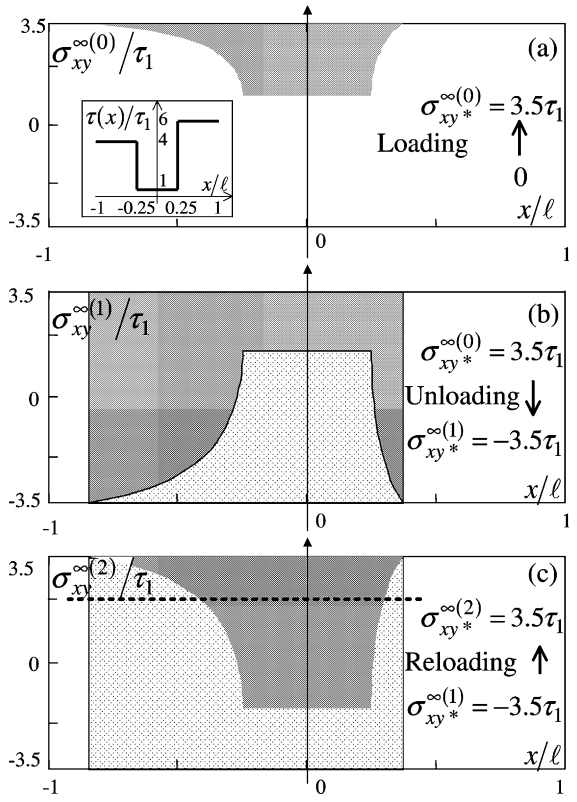

Fig. 3. The case of piecewise constant frictional resistance. Propagation of the sliding zones in the loading (a), unloading (b) and reloading (c) phases.

$(a-\varepsilon_3^{(1)}, b+\varepsilon_2^{(1)})$, until it reaches the ends of the interval $(a-\varepsilon_3^{(0)}, b+\varepsilon_2^{(0)})$. An important observation is that, when the magnitude of the negative stress $\sigma_{xy}^{\infty(1)}$ reaches the level of the peak stress in the loading part of the cycle, the slip accumulated in the mentioned part is fully eliminated (as seen from the fact that the lowest curve of Fig. 4b is a mirror reflection of the upper curve). Thus, at this point, the "memory" of the previous loading stage is fully erased.

Reloading from the state $\sigma_{xy}^{\infty(2)} = \sigma_{xy^*}^{\infty(1)}$ to $\sigma_{xy}^{\infty(2)} = \sigma_{xy^*}^{\infty(0)}$ $(S=2)$. The entire crack remains locked until $\sigma_{xy}^{\infty(2)} = \sigma_{xy^*}^{\infty(1)} + (\tau_1^{(2)}(x) + \tau_1^{(1)}(x))$. When this stress level is reached, a new sliding zone nucleates within (a,b) and, as $\sigma_{xy}^{\infty(2)}$ is increased, it spreads into adjacent intervals $(a-\varepsilon_3^{(2)}, a)$, $(b, b+\varepsilon_2^{(2)})$, where endpoints $\varepsilon_2^{(2)}$ and $\varepsilon_3^{(2)}$ can be found from Eq. (4.2) by setting $\tau_k = \tau_k^{(2)} + \tau_k^{(1)}$, $\varepsilon_k = \varepsilon_k^{(2)}$ and $\sigma_{xy}^{\infty} = \sigma_{xy^*}^{\infty(2)} - \sigma_{xy}^{\infty(1)}$. The intervals with locked (reverse) slip shrink and, at some point, fully disappear (Figs. 3c and 4c).

It is seen that the evolution of the sliding process during reloading is strongly affected by previous loading history (note the difference in the slip distributions (Fig. 5) corresponding to two states at $\sigma_{xy}^{\infty(2)}/\tau_1 = 3.0$ in reloading phase: first—after unloading to negative stress $\sigma_{xy}^{\infty(1)}/\tau_1 = -3.5$ (the dotted line of Fig. 3c) and second—after unloading to $\sigma_{xy}^{\infty(1)}/\tau_1 = 0$).

At the end of the cycle (when the peak stress of the first loading stage $\sigma_{xy^*}^{\infty(0)}$ is reached), the "memory" of the loading history is fully erased: the upper curves of Fig. 4a and c coincide (this phenomenon was called "discrete memory" by Holcomb (1981)). It is important to note that the conclusions drawn from Figs. 3 and 4 apply only to the case when the properties of the system (the profile of the frictional resistance) remain unchanged during the entire cycle (for example, there is no "surface degradation").

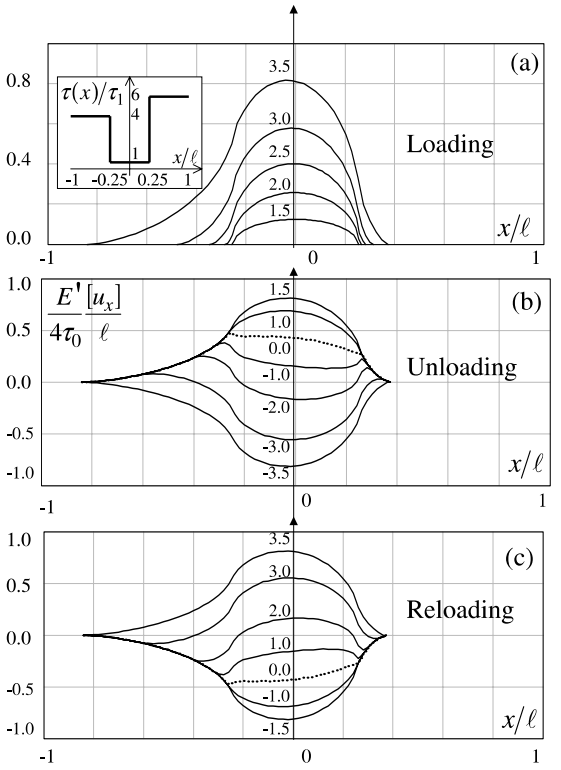

Fig. 4. The case of piecewise constant frictional resistance. Slip distribution in the loading (a), unloading (b) and reloading (c) phases.

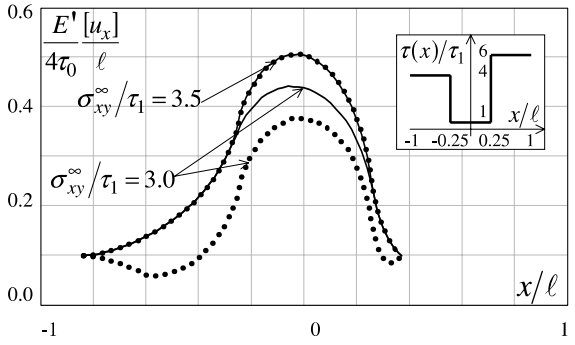

Fig. 5. Stress history dependence of the slip distribution. Dotted and solid lines correspond to the cases when reloading starts at $\sigma^{\infty}_{xy}/\tau_1 = 0$ and $\sigma^{\infty}_{xy}/\tau_1 = -3.5$, correspondingly.

4.2. Influence of changes in the frictional resistance during sliding on the stress–slip behavior

We now consider a more general situation when the profile of the frictional resistance changes during the cycle. Such change may reflect evolution of the sliding surface—slip "weakening" or slip "hardening" (for example, loss of a lubricant in machinery), or changes that are not necessarily related to sliding.

Fig. 6a illustrates the case when the frictional resistance remains unchanged during unloading, but decreases/increases during the reloading part of the cycle (the solid line corresponds to the case of no

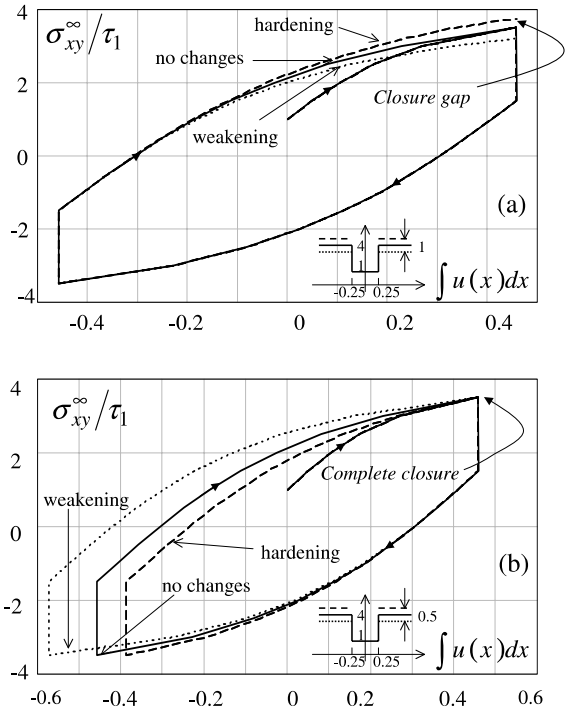

Fig. 6. Impact of changes in the frictional resistance during sliding on the stress–slip behavior of the system; in the reloading (a) and unloading (b) phases of the cycle.

changes). It is seen that the return to the level of the sliding displacement reached during the first loading occurs at decreased/increased levels of the applied load. It appears that this phenomenon has been observed experimentally; see, for example, the data of Olsson (1990).

Fig. 6b illustrates the case when the frictional resistance changes during the unloading part of the cycle, but returns back to the original profile during the reloading part. In contrast with the previous case, the stress–slip loop is fully closed (this implies that the response of the system to a certain subsequent loading will not be affected by the preceding cycle).

4.3. Sensitivity of the stress–slip curves to the profile of frictional resistance

Sensitivity of the sliding process to the profile of frictional resistance (under monotonic loading) was analyzed in detail by Gorbatikh et al. (in press). We now examine how the shape of local minimum of frictional resistance $\tau^{(S)}(x)$ affects the shape of the hysteresis in the stress–slip coordinates (under cyclic loading). This analysis is important for modeling and predicting behavior of different types of systems with observed non-linear responses to the cyclic loading (for example, rock behavior). The assumption of uniform Coulomb's friction that is used mostly in these cases often does not agree with the experimental observations (Olsson, 1984).

Example. A drop of frictional resistance within a certain interval has the triangular shape. We first solve this problem and then compare the results with the case of the step function, with the drop equal to the average value of the triangular profile (Fig. 7a).

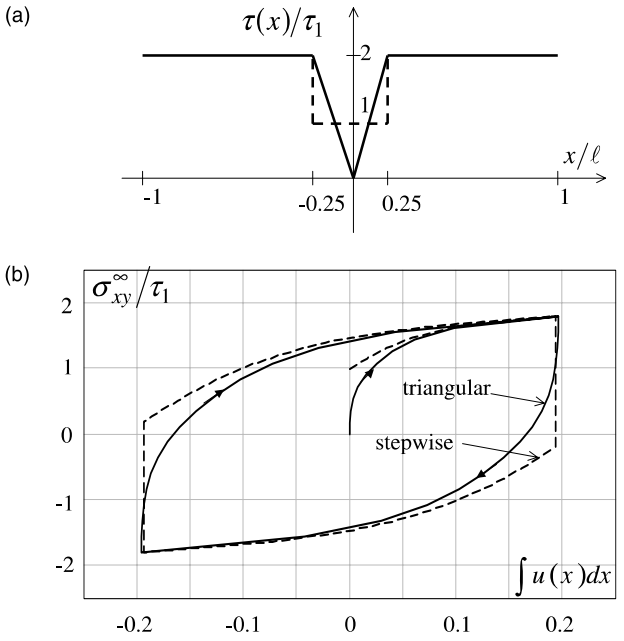

Fig. 7. Sensitivity of the overall slip to the exact profile of frictional resistance in the case of local minimum (triangular minimum is replaced by a stepwise drop having the same average).

Applying the method developed above we obtain the following relations between the applied shear load $\sigma^{\infty(S)}_{xy}$ and the length of the sliding zone $2\varepsilon^{(S)}$, in the case of the triangular shape:

$$\frac{\pi}{2}\frac{\sigma^{\infty}_{xy}-\tau_1}{\tau_2-\tau_1}=\frac{\varepsilon}{a},\quad \varepsilon<a \tag{4.3}$$

$$\frac{\pi}{2}\frac{\sigma^{\infty}_{xy}-\tau_2}{\tau_2-\tau_1}=\frac{\varepsilon}{a}-\sqrt{\frac{\varepsilon^2}{a^2}-1}-\arcsin\frac{a}{\varepsilon},\quad \varepsilon>a \tag{4.4}$$

where $\varepsilon=\varepsilon^{(0)}$, $\tau_k=\tau^{(0)}_k$, $\sigma^{\infty}_{xy}=\sigma^{\infty(0)}_{xy}$ for the loading part of the cycle; $\varepsilon=\varepsilon^{(1)}$, $\tau_k=\tau^{(0)}_k+\tau^{(1)}_k$, $\sigma^{\infty}_{xy}=\sigma^{\infty(0)}_{xy^*}-\sigma^{\infty(1)}_{xy}$ for the unloading part of the cycle; and $\varepsilon_k=\varepsilon^{(2)}_k$, $\tau_k=\tau^{(2)}_k+\tau^{(1)}_k$, $\sigma^{\infty}_{xy}=\sigma^{\infty(2)}_{xy^*}-\sigma^{\infty(1)}_{xy}$ for the reloading phase. Formula (4.3) was derived earlier by Olsson (1984). Fig. 7b illustrates the stress–slip curves for this case (solid line) and for the case when the triangle is replaced by its average value taken over the interval of local minimum of $\tau^{(S)}(x)$. It is seen that the curves almost coincide after the interval of reduced frictional resistance has been already slid. Thus, the "memory" of the interval of reduced τ is retained, essentially, in terms of the average drop only.

5. General solution in the presence of open intervals

We now extend the analysis to the case when open intervals (collectively denoted by $L^{(S)}_3$) are present. By open intervals we mean the intervals (of given, fixed length) where tractions are equal to zero. They model situations where a part of a material has been lost ("fell off") along a certain part of the crack. We emphasize that such traction free intervals are not caused by any system of "prying loads" (as in the work of

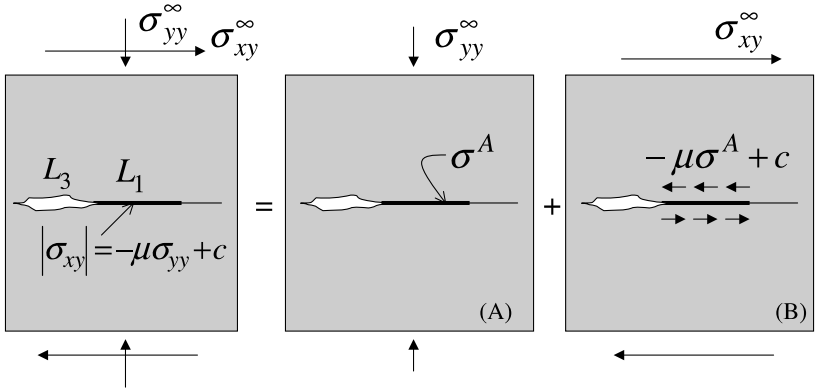

Fig. 8. Stress superposition in presence of open interval L_3 (superscript S is omitted since the superposition holds at any loading step).

Comninou and Dundurs, 1979), but are fixed. In this section Coulomb's law $\tau^{(S)}(x) = -\mu^{(S)}(x)\sigma^{(S)}_{yy}(x) + c^{(S)}(x)$ is assumed along the sliding intervals $L^{(S)}_1$.

Using the stress superposition of Fig. 8, we reduce the problem to two subproblems (A) and (B). Subproblem (A) involves mode I loading only, and traction σ^{A} along interval L_1 is given by the solution of the problem of an open interval under remote compression σ^{∞}_{yy} (and hence may have a singularity if the open interval has sharp tips). Subproblem (B) involves mode II only and can be solved by the method developed by Gorbatikh et al. (in press), briefly overviewed in Section 3. Indeed, reformulating the boundary conditions in terms of function $\Phi(z)$, we have the following formulation of subproblem (B):

$$\Phi^{+}(x) + \Phi^{-}(x) = (-1)^{S+1}\left(\mu^{(S)}(x)\sigma^{\mathrm{A}(S)}_{yy}(x) - c^{(S)}(x)\right)\mathrm{i}, \quad x \in L^{(S)}_1 \tag{5.1}$$

$$\Phi^{+}(x) + \Phi^{-}(x) = 0, \quad x \in L^{(S)}_3 \tag{5.2}$$

$$\Phi^{+}(x) - \Phi^{-}(x) = \frac{2G\delta^{(S)'}(x)}{\kappa + 1}, \quad x \in L^{(S)}_4 \tag{5.3}$$

that is similar to Eqs. (3.2a), (3.2b) and (3.3).

We note that the normal traction distribution $\sigma^{\mathrm{A}(S)}$ depends on whether the endpoint of the open intervals is "sharp" or "blunted". We assume, in the analysis to follow, that the mentioned endpoints are crack tip-like, so that $\sigma^{\mathrm{A}(S)}$ involves a singularity generated at the tip of the open interval by the compressive loading (otherwise, $\sigma^{\mathrm{A}(S)}$ has to be readjusted, in accordance with solutions for stress fields near slender notches).

We also note, that since $\sigma^{\mathrm{A}(S)}$ enters the analysis only via product $\mu^{(S)}(x)\sigma^{\mathrm{A}(S)}$, the singularity at the endpoints of the open interval can, formally, be attributed to $\mu^{(S)}(x)$—these two physically different problems are mathematically identical. Thus, the problem with an open intervals can be reduced to the one considered in the preceding sections, with singular $\mu^{(S)}(x)$.

6. Analysis in presence of an open interval

We now analyze the sliding process in the case of one open interval $(-a, a)$; the analysis can be extended to the case of several open intervals in a straightforward manner. Coulomb's law with cohesion coefficient

$c = 0$ is assumed. We assume that the coefficient of friction—function $\mu^{(S)}(x)$—may change during the loading–unloading cycle.

Thus, sliding starts at a certain point x if the following condition is satisfied there:

$$(-1)^S \sigma_{xy}^{(S)}(x) = \mu^{(S)}(x)\sigma_{yy}^{(S)}(x) \tag{6.1}$$

Stresses $\sigma_{yy}^{(S)}$ and $\sigma_{xy}^{(S)}$ can be taken as induced by an isolated crack with sharp tips (occupying the open interval), loaded by $\sigma_{yy}^{(S)\infty}$ and $\sigma_{xy}^{(S)\infty}$, and evaluated along the interval where the frictional sliding will take place. They are, thus, given by:

$$\sigma_{yy}^{(S)} = \frac{\sigma_{yy}^{(S)\infty}|x|}{\sqrt{x^2 - a^2}}, \qquad \sigma_{xy}^{(S)} = \frac{\sigma_{xy}^{(S)\infty}|x|}{\sqrt{x^2 - a^2}} \tag{6.2}$$

Substituting Eq. (6.2) into Eq. (6.1) leads to cancellation of singular multipliers at the normal and shear terms, so that the condition of nucleation of sliding is re-stated simply as $(-1)^S \sigma_{xy}^{\infty(S)} = \mu^{(S)}(x)\sigma_{yy}^{\infty(S)}$. This condition coincides with the one in absence of the open interval. Therefore, the presence of an open interval produces no effect on the *initiation* of sliding (although it does affect the *propagation* of sliding, as discussed below). This physically interesting observation applies to the case of several open intervals as well.

We now analyze the case when frictional coefficient $\mu^{(S)}(x)$ is piecewise constant on the left and on the right of the open interval (Fig. 9a); in this case the solution can be obtained in closed form and in elementary functions. Cases of other functions $\mu^{(S)}(x)$ can be analyzed by the same method. We consider now the loading ($S = 0$)–unloading ($S = 1$)–reloading ($S = 2$) cycle.

Loading from the initial state $\sigma_{xy}^{\infty(0)} = 0$ to a certain $\sigma_{xy^*}^{\infty(0)}$. Intervals $(-\ell, -a)$ and (a, ℓ) are locked until the applied shear load reaches $\sigma_{xy}^{\infty(0)} = \mu_1^{(0)}\sigma_{yy}^{\infty(0)}$. At this point sliding takes place along the intervals with lowest

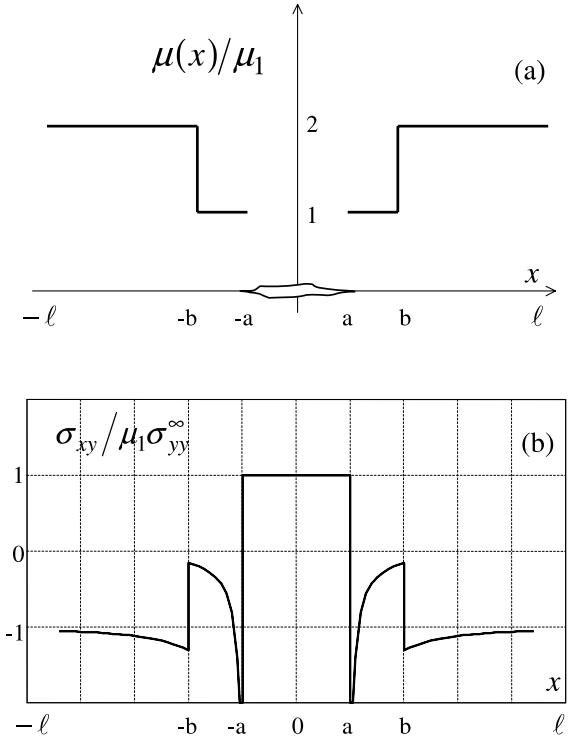

Fig. 9. Frictional coefficient and "driving force" entering K_{II} in presence of open interval $L_3^{(S)}$.

frictional resistance $(-b,-a)$ and (a,b). As $\sigma_{xy}^{\infty(0)}$ is increased, sliding propagates into adjacent intervals $(-h^{(0)},-b)$ and $(b,h^{(0)})$, where $h^{(0)}$ is to be determined. As follows from the superposition of Fig. 8, this problem reduces to the one with one sliding zone $(-h^{(0)},h^{(0)})$, with the following traction distribution (Fig. 9b):

$$\sigma_{xy}=\begin{cases}\sigma_{xy}^{\infty(0)}, & |x|<a\\ \sigma_{xy}^{\infty(0)}+\mu^{(0)}(x)\frac{\sigma_{yy}^{\infty(0)}|x|}{\sqrt{x^2-a^2}}, & |x|>a\end{cases} \tag{6.3}$$

The endpoints $\pm h^{(0)}$ are found from the condition that

$$K_{\mathrm{II}}(\pm h)=-\sqrt{\frac{1}{\pi h}}\int_{-h}^{h}\sigma_{xy}(x)\left\{\frac{h-x}{h+x}\right\}^{\pm 1/2}\mathrm{d}x$$

are equal to zero. This yields the following equation for h:

$$h=\sqrt{\frac{b^2-a^2}{\tan^2 Q}+b^2},\quad \text{where } Q=\frac{\pi}{2}\frac{\tau_2-\sigma_{xy}^{\infty}}{\tau_2-\tau_1} \tag{6.4}$$

with h set equal to $h^{(0)}$ at this stage of loading and $\tau_1=\mu_1^{(0)}\sigma_{yy}^{\infty(0)}$, $\tau_2=\mu_2^{(0)}\sigma_{yy}^{\infty(0)}$, $\sigma_{xy}^{\infty}=\sigma_{xy}^{\infty(0)}$.

Figs. 10a and 11a illustrate propagation of the sliding zones and the corresponding distribution of slip (the displacement discontinuity) along the crack. Note that the displacement discontinuity has the elliptical profile in the open interval.

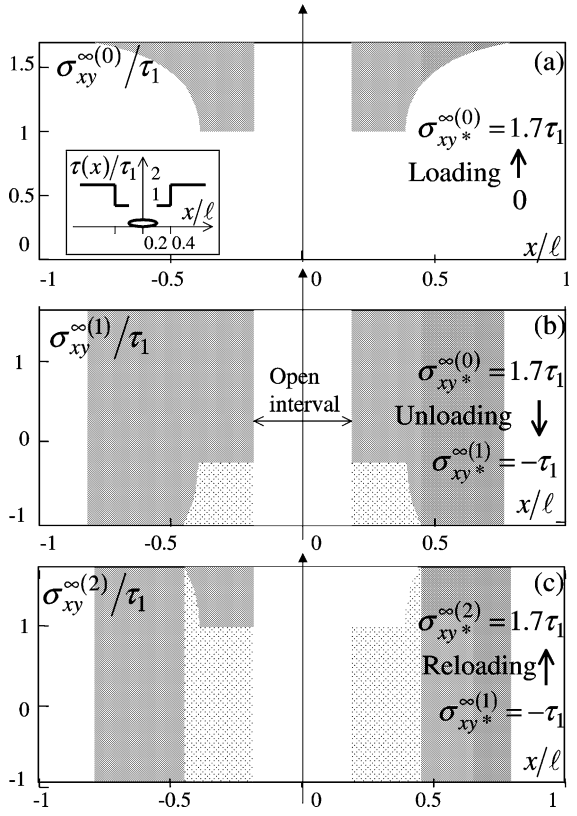

Fig. 10. Propagation of the sliding zones in the loading (a), unloading (b) and reloading (c) phases when one open interval is present. The case of piecewise constant frictional coefficient.

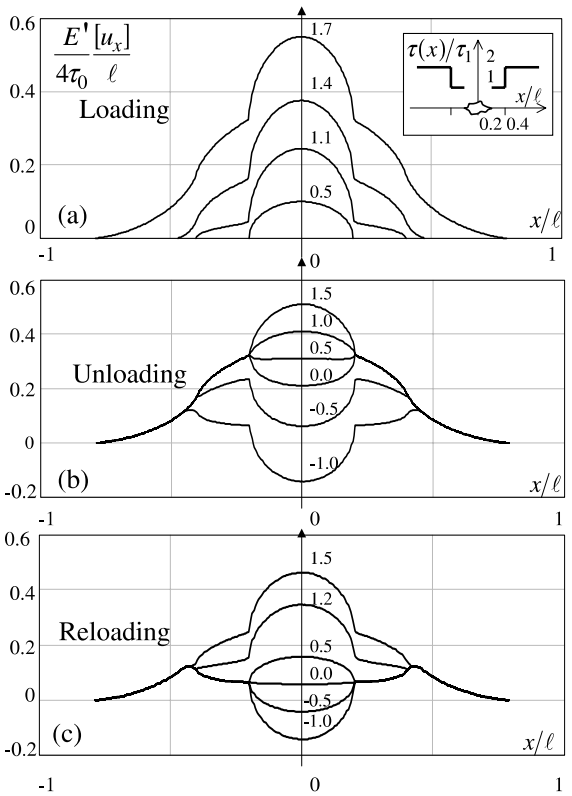

Fig. 11. Slip distribution in the loading (a), unloading (b) and reloading (c) phases when one open interval is present. The case of piecewise constant frictional coefficient.

Unloading from the state $\sigma_{xy}^{\infty(1)} = \sigma_{xy}^{(0)*}$ to $\sigma_{xy}^{(1)*}$. Reverse sliding is preceded by a "deadband"—an interval of loads where no sliding occurs; within this interval the displacement discontinuity over the *open* interval decreases proportionally to the magnitude of applied load $\sigma_{xy}^{\infty(1)}$ (Fig. 11b). The reverse sliding starts when the applied shear load drops to the level $\sigma_{xy}^{\infty(1)} = \sigma_{xy}^{(0)*} - (\tau_1^{(1)} + \tau_1^{(0)})$ (where $\tau_1^{(1)} = \mu_1^{(1)}\sigma_{yy}^{\infty(1)}$ and $\tau_1^{(0)} = \mu_1^{(0)}\sigma_{yy}^{\infty(0)}$) and takes place within $(-b,-a)$ and (a,b). As $\sigma_{xy}^{\infty(1)}$ is further decreased, the reverse sliding propagates into adjacent intervals $(-h^{(1)},-b)$, $(b,h^{(1)})$, where $h^{(1)}$ can be found from Eq. (6.4) by setting $h = h^{(1)}$, $\tau_1 = \mu_1^{(0)}\sigma_{yy}^{\infty(0)} + \mu_1^{(1)}\sigma_{yy}^{\infty(1)}$, $\tau_2 = \mu_2^{(0)}\sigma_{yy}^{\infty(0)} + \mu_2^{(1)}\sigma_{yy}^{\infty(1)}$ and $\sigma_{xy}^{\infty} = \sigma_{xy^*}^{\infty(0)} - \sigma_{xy}^{\infty(1)}$. Figs. 10b and 11b illustrate the propagation of the reverse sliding zone and of the slip distribution, respectively.

Reloading from the state $\sigma_{xy}^{(1)*}$ to the previous peak load $\sigma_{xy}^{(0)*}$. The intervals adjacent to the open interval remain locked until $\sigma_{xy}^{\infty(2)} = \sigma_{xy}^{(1)*} + (\tau_1^{(2)}(x) + \tau_1^{(1)}(x))$ (where $\tau_1^{(1)} = \mu_1^{(1)}\sigma_{yy}^{\infty(1)}$ and $\tau_1^{(2)} = \mu_1^{(2)}\sigma_{yy}^{\infty(2)}$). At this point a new sliding zone nucleates within (a,b). As $\sigma_{xy}^{\infty(2)}$ is increased, this zone spreads into adjacent intervals $(-h^{(2)},-b)$, $(b,h^{(2)})$, where $h^{(2)}$ can be found from Eq. (6.4) by setting $h = h^{(2)}$, $\tau_1 = \mu_1^{(2)}\sigma_{yy}^{\infty(2)} + \mu_1^{(1)}\sigma_{yy}^{\infty(1)}$, $\tau_2 = \mu_2^{(2)}\sigma_{yy}^{\infty(2)} + \mu_2^{(1)}\sigma_{yy}^{\infty(1)}$ and $\sigma_{xy}^{\infty} = \sigma_{xy^*}^{\infty(0)} - \sigma_{xy}^{\infty(1)}$. The intervals with the locked accumulated reverse slip shrink and, at some point, fully disappear (Figs. 10c and 11c); at this point, the memory of the preceding loading step is erased.

A comparison with the case when the open interval is absent shows that *the open interval hinders the propagation of sliding*. This is explained by the fact that the compressive stress has a singularity at the endpoints of the open interval whereas the shear stress does not.

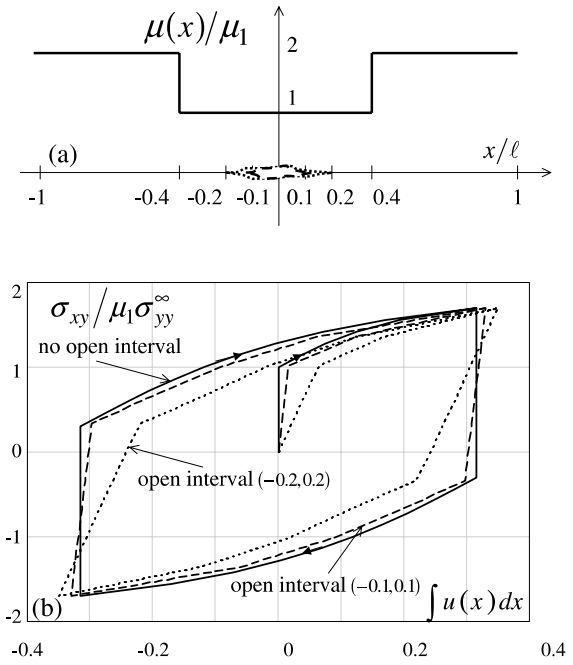

Fig. 12. Stress–slip curves in presence of an open interval (of different lengths). The curve when the open interval is absent is given for comparison.

The influence of the open interval is further illustrated by Fig. 12, where open intervals of two lengths are considered. An interesting observation is that, although the propagation of sliding is hindered by the singularity in σ_{yy} at the tips of the open interval, the total accumulated slip $\int_{-h}^{h}[u(x)]\,\mathrm{d}x$ is larger in the presence of the open interval.

Remark. Although Figs. 10 and 11 illustrate the case simplest when $\mu^{(S)}(x)$ does not change during the sliding process, the solution given above *does* take such changes into account.

7. Discussion and conclusions

Frictional sliding under cyclic loading on a crack with non-uniform frictional characteristics (that may undergo changes in the process of sliding) is analyzed. The contact surface may include "open" intervals of zero tractions that model the situations when some material "fell off" from the sliding zone. The evolution of the sliding zone in the process of stress cycling is analyzed. The basic findings can be summarized as follows.

It is found that the evolution of the sliding process is strongly affected by the preceding loading history. On completion of the stress cycle, the "memory" of the loading history is fully erased (provided the properties of the system—the profile of the frictional resistance—remain unchanged during the cycle).

We examined the impact of changes of the frictional resistance profile $\tau(x)$ in the process of sliding. Such changes may model, for instance, the "degradation" of the sliding contact in the process of sliding, or some other processes that are not necessarily related to sliding. One of the effects of the mentioned changes is that the hysteresis loop in cyclic loading may not close. This phenomenon appears to have been observed experimentally.

We analyzed the sensitivity of the stress–slip curves to the exact profile of the frictional resistance along the crack (this is of importance since the profile is usually not known in exact terms). The analysis is done on the example of a local minimum of the frictional resistance. It is found that, after the zone of the local minimum has been fully slid, the process of further sliding becomes almost insensitive to the exact shape of the minimum. A similar observation holds for the unloading process.

The effect of ''open'' intervals along the crack surface is analyzed. Physically interesting findings are that the onset of sliding is not affected by ''open'' intervals; after sliding started, their presence, on one hand, increases the overall accumulated slip, on the other hand, ''open'' intervals, hinder the *propagation* of sliding.

We note that, similarly to the earlier analysis of Gorbatikh et al. (in press), the results of this work can be extended to the case when the ''open'' intervals are replaced by intervals with a certain prescribed traction distribution. Such a generalization may be relevant to situations involving, for example, fluid pressures along the crack.

Acknowledgements

This work has been supported by NSF and DOE through grants to Tufts University. The first author (LG) acknowledges support of Zonta International Amelia Earhart Fellowship Award.

References

Comninou, M., Dundurs, J., 1979. An example for frictional slip progressing into a contact zone of a crack. Engineering Fracture Mechanics 12, 191–197.

Cooke, M., 1997. Fracture localization along faults with spatially varying friction. Journal of Geophysical Research 102 (B10), 22425–22434.

Gorbatikh, L., Nuller, B., Kachanov, M., 2001. Sliding on cracks with non-uniform frictional characteristics. International Journal of Solids and Structures 38 (42–43), 7501–7524.

Holcomb, D., 1981. Memory, relaxation, and microfracturing in dilatant rock. Journal of Geophysical Research 86 (B7), 6235–6348.

Marone, C., 1998. Laboratory-derived friction laws and their application to seismic faulting. Annual Review of Earth Planetary Science 26, 643–696.

Muskhelishvili, N.I., 1953. Some Basic Problems in the Mathematical Theory of Elasticity. Noordhoff, Groningen-Holland.

Olsson, W., 1984. A dislocation model of the stress history dependence of frictional slip. Journal of Geophysical Research 89 (B11), 9271–9280.

Olsson, W., 1990. The effects of shear and normal stress paths on rock friction. In: Barton, N., Stephansson, O. (Eds.), Proceedings of the International Symposium on Rock Joints. A.A. Balkema, Rotterdam, pp. 475–479.

Pollard, D., Segall, P., 1980. Mechanics of discontinuous faults. Journal of Geophysical Research 85 (NB8), 4337–4350.

Rudnicki, J., Kanamori, H., 1981. Effects of fault interaction on moment, stress drop, and energy release. Journal of Geophysical Research 86 (B3), 1785–1793.

Schultz, R., 1999. Understanding the process of faulting: selected challenges and opportunities at the edge of the 21st century. Journal of Structural Geology 21 (8–9), 985–993.

Weertman, J., 1964. Continuum distribution of dislocations on faults with finite friction. Bulletin of the Seismological Society of America 54 (4), 1035–1058.